07

Autowave Model of an Elastic-Plastic Transition in a Deformable Medium

© L.B. Zuev, V.I. Danilov

Institute of Strength Physics and Materials Science, Siberian Branch, Russian Academy of Sciences, Tomsk, Russia

E-mail: lbz@ispms.ru

Received March 11, 2022
Revised May 16, 2022
Accepted May 18, 2022

The conditions for the generation of autowaves of localized plasticity during the elastic-plastic transition in solids are considered. The similarity and difference between the deformation processes according to the Lüders and Portevin–Le Chatelier mechanisms are analyzed and an explanation of these regularities is proposed, based on the introduction of concepts of active deformable media capable of generating switching autowaves and excitation autowaves. The conditions for the formation of such autowaves and the quantitative characteristics of the processes responsible for the transition to plastic deformation are considered. The relationship between the autowave characteristics and the rate of stretching during mechanical tests has been elucidated.

Keywords: plasticity, dislocations, autowaves, Lüders front, Portevin–Le Chatelier band.

DOI: 10.21883/PSS.2022.08.54695.311

1. Introduction

Phenomenon of plastic deformation of solids continues to be one of the problems in condensed matter physics. The main barrier to understanding its nature is related to the difficulty of understanding the relationship between the micromechanisms of plastic flow, based on dislocation theory and well developed by now [1,2], and the macroscopic patterns of plastic deformation processes [3]. The latter are manifested, in particular, in the non-linearity of the dependence of the deforming stress σ on deformation ε, i.e., in the shape of the plastic flow curve $\sigma(\varepsilon)$.

A solution-oriented model of autowave plasticity [4] considers plastic flow as an evolution of the deformation localization pattern manifested by a change in autowave deformation modes. Experimentally observed autowaves have a macroscopic scale (autowave length), and accounting for their existence provides an explanation for many important laws of plastic flow [5].

The intriguing stage in the development of autowave plasticity is the elastic-plastic transition, after realization of which the autowave mechanisms of the form alteration process are activated, that is, various autowave modes of localized plasticity [4] begin to be generated in a regular manner. Examples of elastic-plastic transitions are the Lüders and Portevin–Le Chatelier deformation processes, whose dislocation mechanisms have been well studied by now [6–9]. With the known differences between these processes, there is a distinct similarity expressed, firstly, in the proximity of the forms of the yield drop and a separate deformation surge and, secondly, in the existence of $\sigma(\varepsilon)$ areas on the flow curves with the strain-hardening coefficient $d\sigma/d\varepsilon < 0$, corresponding to the yield drop or deformation surge.

This paper contains a comparative analysis of the initial development stage of autowave process of plastic flow, i.e., the stage of elastic-plastic transition according to the mechanisms of Lüders or Portevin–Le Chatelier bands nucleation.

2. Lüders and Portevin–Le Chatelier deformations. Experiment

The experimental part of the paper was performed on materials whose deformation clearly shows the named effects. Lüders deformation was studied in alloys Fe−0.08 wt.% C (low carbon steel and ARMCO-iron), and Portevin–Le Chatelier deformation — in alloys Al−4 wt.% Cu and Al−5 wt.% Mg (D1 and AMg5 accordingly). All alloys are deformed by dislocation sliding [6]. Some experiments were performed on polycrystalline titanium nickelide (NiTi), which is deformed by phase transformation B2 → B19′ [10]. Mechanical stretching tests with recording of flow diagram and determination of normal mechanical characteristics such as upper $\sigma_y^{(u)}$ and lower $\sigma_y^{(l)}$ yield strengths, yield point strain (Lüders deformation ε_{pl}) and surge deformation, were synchronized with localized plasticity pattern registration using the digital speckle photographic technique detailed in the monograph [4]. This complemented the mechanical test data with visual information on the development of localized deformation. The combined use of the named techniques made it possible to obtain quantitative data on the patterns of Lüders and Portevin–Le-Chatelier band development, coordinatedly analyzing the plastic flow curves $\sigma(\varepsilon)$ and the time dependences of the band positions, the initial data for which are illustrated in Fig. 1, *a, b*.

One can identify signs of similarity and difference between the macroscopic Lüders and Portevin–Le Chater-

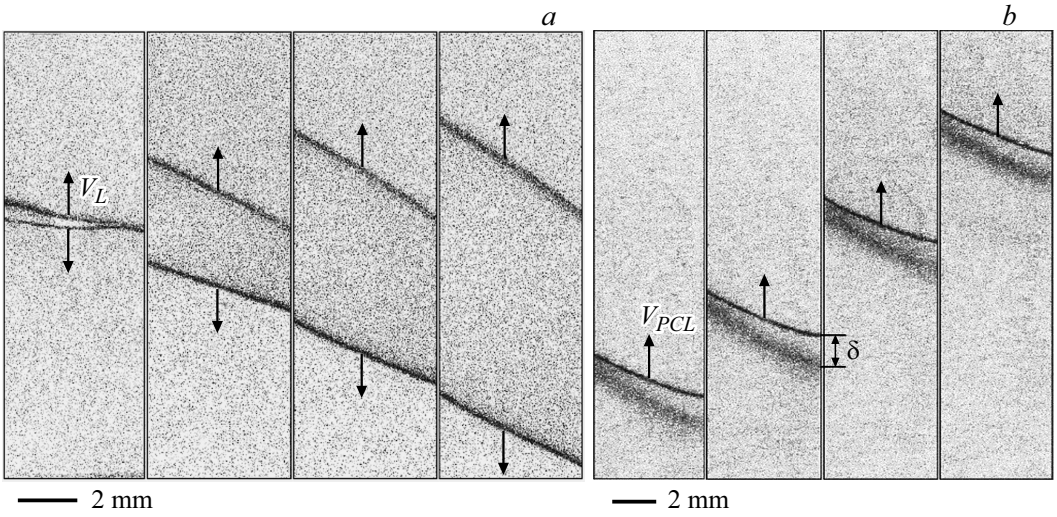

Figure 1. Development of Lüders and Portevin–Le Chatelier deformations. Stretching velocity $1.3 \cdot 10^{-2}$ mm/s, interframe interval 2 s; arrows — directions of fronts. Lüders band propagation in ARMCO-Fe (a); Portevin–Le Chatelier band propagation in AMg5 (b) alloy

.

lier deformation patterns. The similarity of these deformation processes consists in the fact that the growth of bands of both types began with the sprouting of a narrow band nucleus of $\sim 1.5-2$ mm width at rate of $V_{nucl} \approx (1.2-4.0) \cdot 10^{-3}$ m/s through the cross-section of the sample under study. However, further development of Lüders and Portevin–Le Chatelier deformation in the deformed systems followed different scenarios.

Thus development of Lüders band after nucleation consists in its symmetrical expansion (Fig. 1, a), i.e. the simultaneous movement of two Lüders fronts in opposite directions with almost identical velocities $V_L \approx (0.1-7) \cdot 10^{-4}$ m/s, depending on the number of simultaneously developing bands and loading rate during testing. Thus, the width of the Lüders band increases continuously during deformation.

Evolution of Portevin–Le Chatelier band after nucleus formation (Fig. 1, b) is reduced to the movement of its two fronts as a whole along the stretching axis at a constant velocity $V_{PLC} \approx (0.5-3) \cdot 10^{-3}$ m/s, which, like V_L, depends on the deformation rate. At the same time, the distance between the fronts (the width of the Portevin–Le Chatelier band) $\delta \approx 1.5-2$ mm remains constant during the motion. Experimental measurements have shown that the trailing front of the band lags behind the leading one by $t_{del} = \delta/V_{PLC} \approx 1-2$ s.

There is also a noticeable difference in the contrast between the images of the moving fronts of Lüders and Portevin–Le Chatelier. It follows from Fig. 1, a that the two fronts of the same Lüders band have almost the same contrast, while Fig. 1, b shows that the leading front of the Portevin–Le Chatelier band looks significantly more contrasted and narrower compared to the trailing front.

However, apart from the above, the most important difference between Lüders and Portevin–Le Chatelier deformations to be explained is this: Lüders front can pass over the deformed sample only once, after which deformation hardening begins, whereas the Portevin–Le Chatelier bands are able to run over the sample many times during its deformation [6–9].

3. Comparing Lüders and Portevin–Le Chatelier deformations

To understand the reasons for this difference, let us compare the macroscopic patterns of Lüders and Portevin–Le Chatelier deformations with the known literature data on the kinetics of processes in active media, to which the deformed medium [4,11] can be referred. As mentioned above, Lüders front transfers the medium from a metastable elastically deformable state to a stable plastically deformable state. Such a transition can be realized only once in the system, which explains the single passage of Lüders front through the sample. Analysis of the deformation development laws on the yield point during Lüders deformation makes us consider the motion of Lüders front, using the terms of the theory of autowave processes [11], as *autowave switching in a medium of bistable elements*, irreversibly changing the properties of this medium.

The kinetics of the process in Portevin–Le Chatelier deformation turns out to be fundamentally different. In this case, plastic flow begins at the leading front of the band, apparently acting as a switching autowave. The trailing front of Portevin–Le Chatelier band in this case acts as a switching backward autowave [11], terminating deformation and restoring the initial state of the medium. In such a case, a multiple repetition of deformation events is obviously possible. In autowave theory, such a synchronously moving pair of fronts with different roles is considered *to be an excitation autowave in a medium of excitable*

elements [11], after passage of which the initial properties of the medium are restored.

For the proposed explanation, it is possible to introduce quantitative criteria defining the differences of autowave switching and excitation processes for the discussed types of deformation. For this purpose, it is feasible to introduce *refractoriness time* τ_{ref} for them, i.e. the time during which the medium remains indifferent to external influences and only an internally given sequence of transitions [11] occurs therein. Refractoriness time as a natural quantitative characteristic of the autowave process is commonly used for excitation autowaves, but there are no obstacles to extending this concept to switching autowaves. Since the deformation modes in the described experiments for Lüders and Portevin–Le Chatelier deformation are the same, the possible difference in times should reflect the difference in the micromechanisms of the plastic flow.

For Lüders deformation, existence of metastable elastically deformed state at stresses $\sigma < \sigma_y^{(u)}$ is explained by deficit of mobile dislocations because of their blocking by condensed atmospheres of carbon atoms [12]. Stable plastically deformable state occurs after dislocation breaks away from atmospheres at $\sigma = \sigma_y^{(u)}$. In this case the refractoriness time may be the period required for repeated blocking of released dislocations by condensed atmospheres (time of post-deformation ageing [12]). This process is controlled by diffusion of carbon to dislocations in the mesh α-Fe, and its duration may be assessed using a known diffusion ratio

$$\tau_{ref}^{(L)} \approx \frac{(\Lambda)^2}{2D_C} \approx \frac{\rho^{-1}}{2D_C}, \qquad (1)$$

where $\rho = 10^{14}\,\mathrm{m}^{-2}$ — density of dislocations [12], which determines diffusion wave by ratio $\Lambda = \rho^{-1/2}$. At $T = 300\,\mathrm{K}$ carbon diffusion coefficient in α-Fe $D_C \approx 5.6 \cdot 10^{-21}\,\mathrm{m}^2/\mathrm{s}$ [13], so that in accordance with equation (1), blocking is restored for the refractoriness time of Lüders deformation $\tau_{ref}^{(L)} \approx 10^6\,\mathrm{s}$. It must be compared to specific time of experiment, for example, with specific time of Lüders front passage along sample length $t_{exp} \approx 10^2 - 10^3\,\mathrm{s}$, measured in experiments. Besides, for all cases of Lüders deformation $\tau_{ref}^{(L)} \gg t_{exp}$ or $\tau_{ref}^{(L)}/\tau_{exp} \gg 1$. This means that the deformed medium does not have time to return to the initial state during the experiment, and for this reason, the Lüders front passage through the sample is performed only as a single act.

To estimate refractoriness time of Portevin–Le Chatelier process, it is not necessary to use the dislocation models [7–9] available in the literature. Here we can use the value $t_{del} = \delta/V_{PLS} \approx 1-2\,\mathrm{s}$ as the refractoriness time, assuming that $\tau_{ref}^{(PLS)} \approx t_{del}$. Fairness of such conclusion is justified by the fact that the elastic properties of the medium are restored after Portevin–Le Chatelier band trailing front has passed through it. This is indicated by invariability of deformation surge shape during subsequent passages of the Portevin–Le Chatelier bands. Small refractoriness time explains the multiple deformation surges by the fact that at the leading front of Portevin–Le Chatelier bands the dislocations become mobile, while at the trailing front the initial state of the medium is restored. Such a process can be repeated many times. Difference in the structure of the leading and trailing fronts (Fig. 1, *b*) is related to their different role in deformation.

It is then obvious that the condition $\tau_{ref}^{(PLC)} \ll \tau_{exp}$ or $\tau_{ref}^{(PLC)}/\tau_{exp} \ll 1$ is fulfilled in the Portevin–Le Chatelier deformation. We can assume that inequalities $\tau_{ref}^{(L)}/\tau_{exp} \gg 1$ and $\tau_{ref}^{(PLC)}/\tau_{exp} \ll 1$ are the criteria by which the system chooses alternative realizations of Lüders or Portevin–Le Chatelier effects. Different nature of autowave flow processes during these effects is a consequence of different refractoriness times of the processes, i.e., the inequality $\tau_{ref}^{(L)} \gg tau_{ref}^{(PLC)}$. In turn, absolute values of refractoriness times are determined by the different nature of microscopic dislocation acts of plastic deformation for the cases under consideration.

To verify these considerations, deformation experiments were performed at $T = 400\,\mathrm{K}$. At this temperature, carbon diffusion coefficient increases to $D_C \approx 2.4 \cdot 10^{-17}\,\mathrm{m}^2/\mathrm{s}$, and refractoriness time calculated from equation (1) decreases accordingly to $\tau_{ref}^{(L)} \gg 4 \cdot 10^2\,\mathrm{s}$. This value is commensurate with $t_{exp} \approx 10^2 - 10^3\,\mathrm{s}$, and condition $\tau_{ref}^{(L)} \gg t_{exp}$ is changed to equality $\tau_{ref}^{(L)} \approx t_{exp}$. In full accordance with this estimation, deformation of Fe-C alloy on the yield point at $T = 400\,\mathrm{K}$ results in a surge-like deformation, i.e., the Portevin–Le Chatelier type effect is realized.

4. Quantitative patterns of Lüders deformation

When several Lüders bands nucleate and develop in a sample simultaneously or sequentially, the rule is followed for them,

$$\sum_{i=1}^{N} |V_L^i| = V_\Sigma = \mathrm{const}, \qquad (2)$$

where $|V_L^i|$ — velocity modulus of the i-moving Lüders front, and N — number of simultaneously moving fronts. According to the experimental results obtained, value of the constant V_Σ in equation (2) depends on the rate of sample stretching V_{mach}. Nucleation of new Lüders bands in the course of deformation at $V_{mach} = \mathrm{const}$ is accompanied by such autotuning of existing fronts velocities that the rule (2) is satisfied. Obviously, the rule is equivalent to the condition of constancy of the growth rate of the plastically deformed area during Lüders deformation.

Explanation of the meaning of rule (2) is based on natural assumption that the total plastic deformation growth in the two fronts produced by the formation of a single Lüders band may not be sufficient to maintain the constant deformation rate given by the testing machine. In such

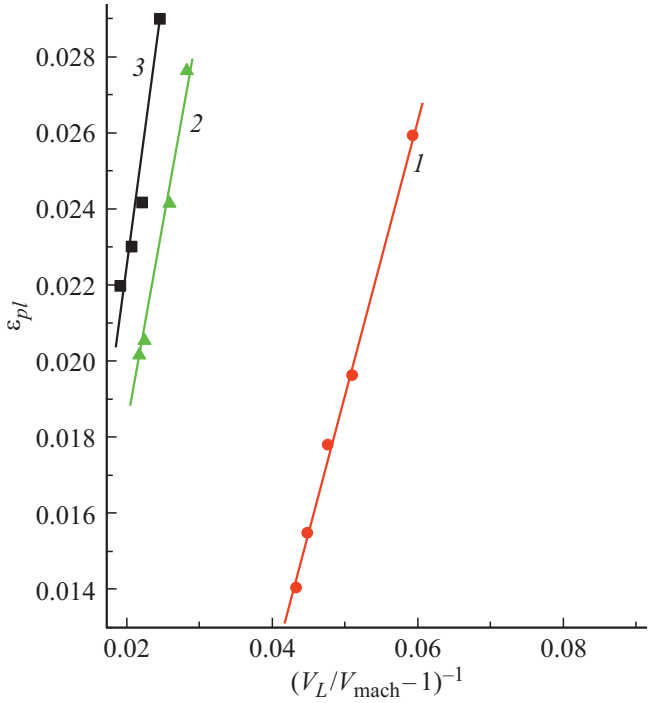

Figure 2. Dependence of Lüders deformation on stretching velocity; NiTi (*1*), Fe (*2*), ARMCO-Fe (*3*).

a case, the medium to be deformed must either collapse or generate new Lüders bands and, consequently, new deformation fronts. Cumulative deformation in the new set of fronts ensures the steady development of the plastic flow process.

As shown by experimental results, kinetic characteristics of the bands and Lüders fronts depend on stretching velocity of the test V_{mach}. A formal relationship between the velocities V_L and V_{mach} can be established by equating the front travel time along the sample length $(L+\delta L)/V_L$ to the time it takes to lengthen sample $\delta L/V_{mach}$. Here L — initial length of the sample, and δL — its absolute elongation when deformed by Lüders. Assuming that Lueders deformation $\varepsilon_{pl} \approx \delta L/L$, we obtain

$$\frac{L+\delta L}{V_L} = \frac{\delta L}{V_{mach}}. \tag{3}$$

Since $\delta L \ll L$, ratio (3) can be written as

$$V_L \approx \left(1+\frac{L}{\delta L}\right)V_{mach} \approx (1+\varepsilon_{pl}^{-1})V_{mach}. \tag{4}$$

Usually $0.01 \le \varepsilon_{pl} \le 0.03$, that is, $V_L \approx (10-30)V_{mach}$, which corresponds to observed Lüders front velocities in experiments [6,14–16]. At the same time Lüders deformation and stretching velocity are linearly related, and the experimentally found ratio for iron looks like

$$\varepsilon_{pl}^{(\text{Fe})} = 0.02 + \frac{V_{mach}}{V_0^{(\text{Fe})}}, \tag{5}$$

where $V_0^{(\text{Fe})} \approx 0.6 \cdot 10^{-3}$ m/s. For titanium nickelide this dependence looks like

$$\varepsilon_{pl}^{(\text{NiTi})} = 0.014 + \frac{V_{mach}}{V_0^{(\text{NiTi})}}, \tag{6}$$

where $V_0^{(\text{NiTi})} \approx 1.1 \cdot 10^{-3}$ m/s. Constants $V_0^{(\text{Fe})}$ and $V_0^{(\text{NiTi})}$ in ratios (5) and (6) by order of value are close to experimental values of Lüders bands nuclei growth velocities in Fe and NiTi, i.e. $V_0^{(\text{Fe})} \approx V_0^{(\text{NiTi})} \approx V_{nucl}$.

To confirm nature of linear dependences (6) and (7), let us solve equation (5) relative to Lüders deformation ε_{pl}

$$\varepsilon_{pl} = \frac{1}{V_L/V_{mach}-1}. \tag{7}$$

Functions $\varepsilon_{pl}(V_{mach})$ are shown in Fig. 2 in coordinates $\varepsilon_{pl} - (V_L/V_{mach}-1)^{-1}$. Since $V_L/V_{mach} \gg 1$, from equation (7), as in [16], $\varepsilon_{pl} \sim V_{mach}$ follows.

Dependence of observed Lüders fronts n_f on loading velocity shown on Fig. 3, *a* also finds explanation in the autowave plasticity model. Saturation of dependence $n_f(V_{mach})$ at $n_f \approx 5$ is related to existence of minimum size of medium λ, where dissipative (localization) structures [17] may arise. This size is determined by equality of autowave process period and specific diffusion time, which results in simple ratio of „diffusion“ type $\lambda \approx (2\Upsilon\tau)^{1/2}$. It includes specific time of autowave process of plastic deformation $\tau \approx 10^3$ s and transport coefficient of local deformation redistribution in plastically deformed medium $\Upsilon \approx 10^{-7}$ m^2/s [4]. Estimation gives $\lambda \approx 10^{-2}$ m, and since working length of samples $\sim 5 \cdot 10^{-2}$ m, the maximum number of Lüders fronts, which could be observed at such experiment conditions, $n_f \le 5$. From Fig. 3, *b* it follows that ascending branch of dependence $n_f(V_{Mach})$ looks like $\ln(1-n_f/5) \sim V_{Mach}$, i.e.

$$n_f \sim \text{const} - \exp\left(-\frac{V_{mach}}{V_0}\right). \tag{8}$$

Here, as shown above when discussing equations (5) and (6), $V_) \approx V_{nucl}$, which underlines relationship of kinetic parameters of Lüders fronts.

To determine specific type of Lüders front velocity dependence on sample stretching velocity, several experiments were conducted on materials, deformation of which is implemented to form Lüders bands and fronts (Fe, ARMCO-Fe, NiTi). Dependences $V_L(V_{mach})$ produced in these experiments and shown on Fig. 4 are approximated by weakly non-linear function

$$V_L = KV_{mach}^n = K'\left(\frac{V_{mach}}{V_0}\right)^n, \tag{9}$$

where parameter $\langle n \rangle = 0.9 \pm 0.1 < 1$ is averaged by three investigated materials. In equation (9) empirical coefficient $K' = KV_0^n \approx 0.04$ m/s, if one believes, as above, that $V_0 \approx V_{nucl} \approx 10^{-3}$ m/s.

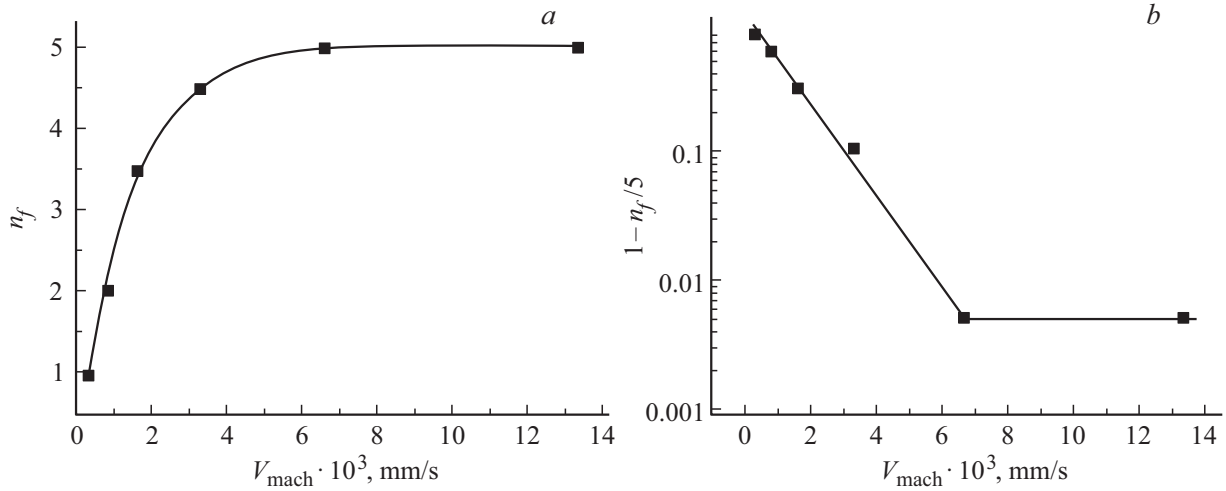

Figure 3. Dependence of number of Lüders fronts in Fe on stretching rate: in coordinates $n_f - V_{mach}$ (a); in coordinates $\ln(1 - n_f/5) - V_{mach}$ (b).

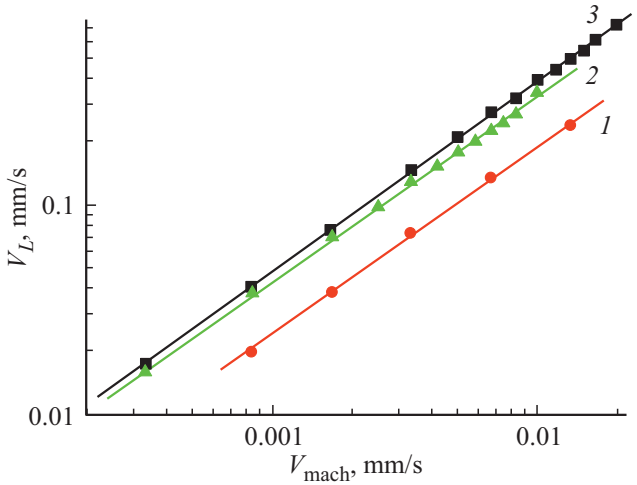

Figure 4. Lüders front motion velocity depending on loading velocity: NiTi (*1*), Fe (*2*), ARMCO-Fe (*3*).

To explain physical nature of detected non-linearity of function $V_L(V_{mach})$, let us characterize growth of Lüders front dV_L in increase of stretching velocity by dV_{mach} of derivative dV_L/dV_{mach}. Let it, as in [18], this derivative is proportionate to ratio of energy flows dissipated in motion of Lüders front $N_L = \sigma_y^{(l)} V_L$ at lower yield point at $\sigma = \sigma_y^{(l)}$ and arriving from loading device $N_{mach} = \sigma_y^{(u)} V_{mach}$ at upper yield point at $\sigma = \sigma_y^{(u)}$. Then,

$$\frac{dV_L}{dv_{mach}} \sim \frac{N_L}{N_{mach}} = \frac{\sigma_y^{(l)} V_L}{\sigma_y^{(u)} V_{mach}}. \tag{10}$$

It is easy to see that in the right part of equation (10) size of products $[\sigma \cdot V] = (\mathrm{N} \cdot \mathrm{m}^{-2}) \cdot (\mathrm{m} \cdot \mathrm{s}^{-1}) = \mathrm{J} \cdot \mathrm{m}^{-2} \cdot \mathrm{s}^{-1}$ actually complies with energy flows. Separating variables in equation (10), we get equation

$$\frac{dV_L}{V_L} \sim \frac{\sigma_y^{(l)}}{\sigma_y^{(u)}} \frac{dV_{mach}}{V_{mach}}, \tag{11}$$

from which the ratio follows

$$\ln V_L \sim \frac{\sigma_y^{(l)}}{\sigma_y^{(u)}} \ln V_{mach}, \tag{12}$$

leading to parabolic dependence $V_L \sim V_{mach}^m$. For indicator m one may accept that

$$m = \frac{\sigma_y^{(l)}}{\sigma_y^{(u)}} < 1, \tag{13}$$

since $\sigma_y^{(l)} < \sigma_y^{(u)}$. Value $\langle m \rangle = \langle \sigma_y^{(l)} / \sigma_y^{(u)} \rangle = 0.94 \pm 0.03$ averaged by data of all conducted experiments may be compared to the above value of indicator $\langle n \rangle = 0.9 \pm 0.1$ in equation (9). For this purpose it is necessary to apply the standard statistical procedure of averages — Fig. 4. Lüders front motion velocity depending on loading velocity: NiTi (*1*), Fe (*2*), ARMCO-Fe (*3*) [19]. It turned out that difference in indicators $\langle n \rangle$ and $\langle m \rangle$ is statistically negligible, so that use of ratio $\langle n \rangle = \langle \sigma_y^{(l)} / \sigma_y^{(u)} \rangle$ is permissible. Such estimates confirm results produced by authors [16] who believed that $V_L \sim V_{mach}$.

5. Conclusion

Consistent development of autowave representations about the nature of plastic flow made it possible to explain the difference in the kinetics of Lüders bands and Portevin–Le Chatelier bands development and to demonstrate that it is associated with the difference in mechanisms of active deformed media response to external mechanical influence.

This difference entails bistability of the deformed medium with the possibility of Lüders band nucleation or excitability of the medium capable of generating Portevin–Le Chatelier bands.

Accordingly, Lüders deformation is equivalent to generation and propagation of a switching autowave in a sample. Portevin–Le Chatelier deformation, which differs from it, can be interpreted as the propagation of the excitation autowave in the deformed medium.

In quantitative sense, bistable and excitable media and, accordingly, switching and excitation autowaves are characterized by different refractoriness times, which, in turn, are uniquely determined by the micromechanisms of elementary plasticity acts in deformable materials. Thus, a quantitative relationship between autowave and dislocation models of plastic flow is established. The developed approach also makes it possible to explain alteration of deformation modes, for example, when temperature changes, and to understand the nature of a number of quantitative dependences characteristic of the kinetics of Lüders and Portevin-Le Chatelier bands.

Funding

The paper was prepared as part of the state assignment of the Institute of Strength Physics and Materials Science of the Siberian Branch of the Russian Academy of Science, subject No. FWRW-2021-0011.

Conflict of interest

The authors declare that they have no conflict of interest.

References

[1] U. Messerschmidt. Dislocation Dynamics during Plastic Deformation. Springer, Berlin (2010). 503 p.
[2] A. Argon. Strengthening Mechanisms in Crystal Plasticity. University Press, Oxford (2008). 404 p.
[3] A. Ishii, S. Ogata. Int. J. Plasticity **8**, 32 (2016).
[4] L.B. Zuev. Avtovolnovaya plastichnost. Lokalizatsiya i kollektivnye mody. Fizmatlit, M. (2018). 207 p. (in Russian).
[5] L.B. Zuev, S.A. Barannikova, V.I. Danilov, V.V. Gorbatenko. Prog. Phys. Met. **22**, 3 (2021).
[6] J. Pelleg. Mechanical Properties of Materials. Springer, Dordrecht (2013). 634 p.
[7] G.A. Malygin. FTT **34**, 2356 (1992). (in Russian).
[8] A.A. Shibkov, M.F. Gasanov, M.A. Zheltov, A.E. Zolotov, V.I. Ivolgin. Int. J. Plasticity **86**, 37 (2016).
[9] A.C. Iliopulos, N.S. Nikolaidis, E.C. Aifantis. Physica A **438**, 506 (2015).
[10] K. Otsuka, X. Ren. Prog. Mater. Sci. **50**, 511 (2005).
[11] A.Yu. Loskutov, A.S. Mikhailov. Osnovy teorii slozhnykh sistem. IKI, M.- Izhevsk (2007). 612 p. (in Russian).
[12] A.H. Kottrell. Dislokatsii i plasticheskoe techenie v kristallakh. Metallurgizdat, M. (1958). 267 p. (in Russian).
[13] C.A. Wert. Phys. Rev. **79**, 601 (1960).
[14] P.Y. Manach, S. Thuillier, J.W. Yoon, J. Coër, H. Laurent. Int. J. Plasticity **58**, 66 (2014).
[15] J.F. Hallai, S. Kyriakidis. Int. J. Plasticity **47**, 1 (2013).
[16] H.B. Sun, F. Yoshida, M. Ohmori, X. Ma. Mater. Lett. **57**, 4535 (2003).
[17] G. Nikolis, I. Prigozhin. Samoorganizatsiya v neravnovesnykh sistemakh. Mir, M. (1979). 512 p. (in Russian).
[18] F.R.N. Nabarro. Phys. Solid State. **42**, 1417 (2000).
[19] D. Hudson. Statistika dlya fizikov. Mir, M. (1967). 242 p. (in Russian).